

PAPER • OPEN ACCESS

Graphenic carbon as etching mask: patterning with laser lithography and KOH etching

To cite this article: A Furio *et al* 2019 *J. Phys.: Conf. Ser.* **1226** 012011

View the [article online](#) for updates and enhancements.



IOP | ebooks™

Bringing together innovative digital publishing with leading authors from the global scientific community.

Start exploring the collection—download the first chapter of every title for free.

Graphenic carbon as etching mask: patterning with laser lithography and KOH etching

A Furio^{1,2}, M Stelzer¹, M Jung¹, H C Neitzert², F Kreupl¹

¹ Technical University of Munich (TUM), Arcistr. 21, Munich, Germany

² University of Salerno, Via Giovanni Paolo II 132, Fisciano, Italy

E-mail: furioalfonso@gmail.com

Abstract. The wet anisotropic etching process is generally used in the field of micromachining (MEMS), particularly for commercial products such as accelerometers. Hard masks like oxide or nitride play a key role in the transfer of patterns to the substrate during the lithography process. This work reports on the use of polycrystalline graphenic carbon as an etch mask for wet chemical processing and outlines a simple method to create patterned structures on (100) silicon wafers. Graphenic carbon (GC) was deposited on the silicon substrate by chemical vapor deposition (CVD) using C₂H₄ as precursor. The desired pattern was written in the spin-coated negative photoresist using UV laser lithography. Different geometrical shapes were printed on the substrate with dimensions ranging from 10 to 50 micrometers. In the next stage, the O₂ plasma etched away the carbon from the area not covered by the photoresist, acting as an additional mask for this and the subsequent processing steps. Finally, the sample was immersed in the KOH bath saturated with isopropanol and the etching rate was evaluated for each crystal plane. Compared to the use of a sacrificial oxide mask, this technique is simpler and produces more reliable results.

1. Introduction

Anisotropic wet etching is one of the most used techniques for fabricating 3D structures as MEMS on silicon substrates. Particularly, bulk etching is widely used to remove silicon from the substrates in order to produce sensors or actuators. Typical micromechanical devices, manufactured on (100) silicon wafer, are cantilevers or membranes that usually need supporting structures based on oxides or nitrides [1]. These insulating hard masks also play an important role during the lithography step for transferring patterns to the substrates. The etching process is usually carried out in an aqueous solution of KOH, but as reported by Barycka et al. [2], the KOH solution saturated with isopropyl alcohol is the most frequently used to obtain a high etch rate ratio and smooth surface on (100) silicon. The choice of the etching solution depends on different factors such as etch rate and anisotropy. The etch rate differs between the crystal planes and the concentration of the used solution [3, 4]. The aim of this work is to create 3D structures on (100) silicon wafer using photolithography and wet anisotropic etching in a commonly used solution of KOH and isopropanol. In this context, the use of graphenic carbon (GC) [5, 6] as an etching mask instead of sacrificial oxide is a new feature. As reported in [7, 8], it is possible to form GC membranes on one side of a wafer exploiting the undercut created by the KOH (saturated with isopropanol) on a silicon substrate. GC is a good candidate for the future process due to the fact that it is inert to most common solvents such as acetone and NMP



and, with a thickness of a few nanometers, it is resistant to HF and KOH. Another advantage is that it is extremely easy to remove with a O₂ or H₂ plasma and that it is compatible with the CMOS standard process through chemical vapor deposition (CVD). Moreover, the thickness of the GC is easily tunable by controlling the parameter of the deposition. The high-temperature stability, the low contact resistance to silicon and the endurance to high current densities make this material the ideal candidate for metal-silicon contacts [9]. In the process flow of this work, this means saving process steps using a conductive mask.

2. Sample preparation

The substrate used for this work is a n-type silicon wafer, doped with arsenic ($\rho = 0.01 \Omega\text{cm}$) covered by an epitaxial layer with a thickness of 8 μm , doped with phosphorus ($\rho = 0.75 \Omega\text{cm}$). The crystallographic orientation of the surface is in the (100) plane. The wafer used for the samples was cut in pieces of 1 cm x 1 cm with a thickness of $625 \pm 25 \mu\text{m}$.

2.1. Substrate cleaning

During the fabrication process, the contamination of particles on the surface of the wafer needs to be avoided in order to have a clean substrate for the further steps. A smooth and clean surface is necessary to deposit effectively a uniform graphenic carbon film. First, the sample was placed in acetone at 60 °C and sonicated for 10 min, in order to remove the protective resist layer. Next, the sample was put into isopropyl alcohol and sonicated with the same previously reported conditions to remove the acetone residuals not soluble in water. Afterward, the sample was prepared with a full RCA clean [10]. The standard cleaning SC-1 was done at 75 °C for 10 min to eliminate the organic residuals. After that, the standard cleaning SC-2 was performed at 75 °C for 10 min to remove ionic contaminations due to metallic particles on the surface.

2.2. Graphenic carbon deposition

Before the carbon deposition, it is necessary to dip the sample in 5% hydrofluoric acid (HF) for 150 sec to remove the native oxide. The deposition was performed with a low-pressure chemical vapor deposition (LPCVD) process at 1000 °C. The used precursor was C₂H₄ with a gas flow of 20 sccm and the pressure in the chamber was 20 mbar. This deposition was carried out for 7 min to obtain the desired layer of GC [6, 9].

2.3. Laser lithography

The lithography process is used to transfer the patterns to the substrate using a spin-coated negative photoresist and a UV laser. Firstly, the sample was heated on a hotplate up to 200 °C for 30 min to remove the adsorbed humidity and afterward, the resist ma-N 1420 was spin-coated on the cooled substrate at 3300 rpm for 30 sec. Next, the sample was heated for 90 sec at 100 °C to remove the solvents from the resist. In order to generate the desired structure, the surface of the sample was exposed to the focused laser beam of the *KLOÉ Dilase 250* laser writer with a laser wavelength of 375 nm and a power density of 351 kW cm⁻². Fig. 1 shows the process steps and the result after the laser lithography. The key parameters to control the design are the modulation of the laser intensity, the velocity of the stage, the focal plane, the exposure time and the possibility to apply three different optical filters. The minimum spot size of the laser is 1 μm but changing the focal plane a spot size around 100 μm has been obtained. The writing process requires only few minutes to produce more than hundreds of reproducible shapes using velocity and repositioning velocity of 2 mm s⁻¹. Finally, the sample was dipped in ma-D 533/s, which is a developer that removes the unexposed resist in around 1 minute. This developing time is particularly critical and can directly affect the geometric property and the resolution of the pattern.

2.4. Dry etching

The RF plasma process was used to remove the carbon from the area that is not covered by the resist. The pressure in the chamber was 2 mbar for a H_2 plasma and around 0.5 mbar for a O_2 plasma respectively. The effects of both plasmas were compared and evaluated under different conditions. The etching time was always set at 3-times 10 sec with 30 sec of cooling time. In the Fig. 2, the process steps and the result are shown. After the plasma etching, the resist was removed as reported in Sec. 2.1.

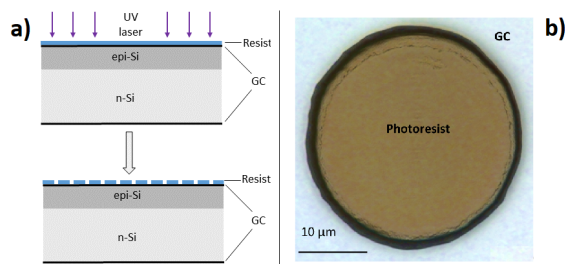


Figure 1. Certain areas of the surface are exposed to the focused laser beam to generate the desired pattern (a). An example of the exposed and developed circular resist pattern is shown in (b).

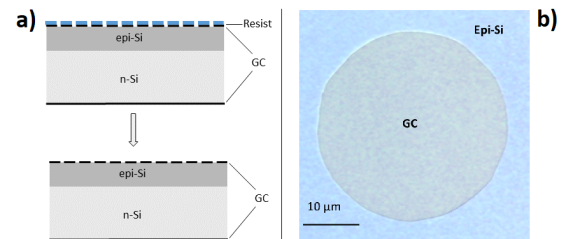


Figure 2. After the development of the resist, the pattern is created in the carbon by etching the carbon away. The process steps are illustrated in (a). (b) shows an optical true color image of a structure after removal of the resist.

2.5. Wet etching

Before being dipped into the KOH bath, the sample was immersed into HF for 30 sec to remove the native oxide that could delay the silicon etching. A 5 M solution of KOH saturated with isopropanol was heated up at $80^\circ C$ in a constant-temperature water bath and the sample was immersed for 9 min. After that, decontamination with the SC-2 cleaning was carried out for 30 min. The final result of this step and the relative schematic is reported in Fig. 3.

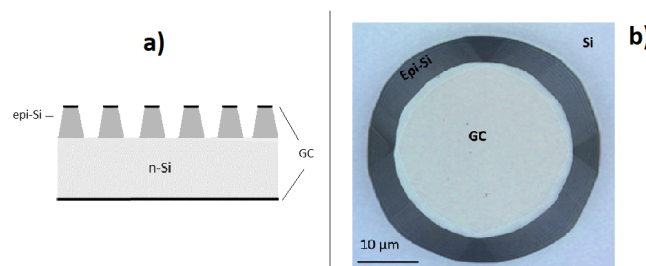


Figure 3. After the pattern of the carbon layer by plasma etching, the native oxide was removed by a HF bath and the silicon was etched away using KOH saturated with isopropanol. a) Shows a schematic of the wet etching result. b) (top view) 3D laser image of the circular structure after the wet etching process.

3. Results

In order to determine the presence of the GC on the substrate, Raman spectroscopy is used with a laser excitation at 532 nm. The D and G bands are the most relevant ones for the GC

spectrum and are shown in Fig. 4.

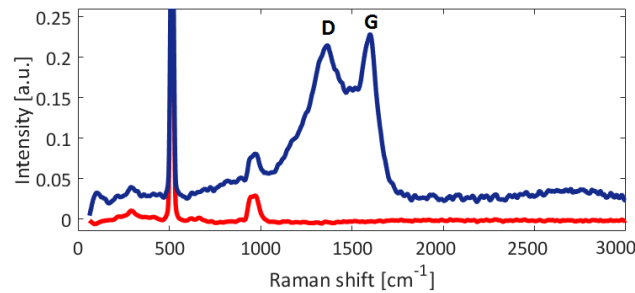


Figure 4. Raman spectra of GC after a deposition of 33 nm on silicon substrate (blue) and silicon without GC (red).

The Raman shift associated with the D and G peaks are at 1350 cm^{-1} and 1584 cm^{-1} . As reported by [11], the high content of covalent sp^2 -bonds is highlighted by the height of the G peak compared to the D peak. After the plasma dry etching, the GC is removed and the two silicon peaks at 520 cm^{-1} and 960 cm^{-1} are clearly visible. After the GC deposition, as described in Sec. 2.2, the surface roughness of the film was measured with an atomic force microscopy (AFM) set in tapping mode in order to not damage the surface. The root mean square height (S_q) is $1.3 \pm 0.1\text{ nm}$ and the dashed white line in the Fig. 5 (a) shows the section where the profile of the film was evaluated. The thickness of the GC was measured with a 3D laser microscope (*Keyence VK series*) on a sample patterned with lines and crosses through the laser lithography and after the removal of the carbon from the area not covered by the resist by dry etching. In this way, a step to evaluate the height of the GC deposition was obtained. The dashed black line in the Fig. 6 (a) shows where the analysis was taken and the Fig. 6 (b) shows the step with the height of $33 \pm 1\text{ nm}$.

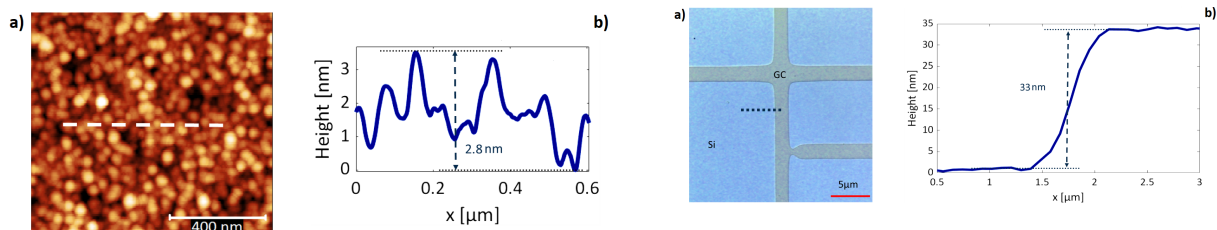


Figure 5. a) AFM image of a silicon sample after a deposition of GC. b) AFM profile of GC.

Figure 6. a) 3D laser microscope image of a GC cross. b) Cross profile to determine the thickness of the GC deposition.

Concerning the laser lithography, the resist used has a thickness of $2\text{ }\mu\text{m}$ using the spin coating parameters reported in Sec. 2.3. It was investigated how to obtain different diameters during the writing process by setting the focal plane, the exposure time and the modulation. In the plot (a) of the Fig. 7 the diameter function of the exposure time for different focal planes, at fixed modulation (80%) and without a filter it is shown. In the plot (b) of Fig. 7 the exposure dose function of the exposure time at a different focal plane and at fixed modulation it is illustrated.

The value of the exposure dose D was evaluated according to the following equation:

$$D = \frac{P \cdot m}{(\pi r^2)} \cdot t \quad (1)$$

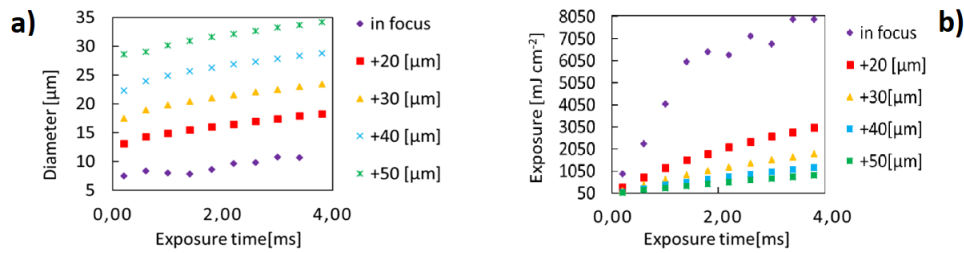


Figure 7. a) Experimental plot of the dot diameters function of the exposure time at fixed modulation and focal plane. b) Plot of the exposure dose transferred to the resist, function of the exposure time, at fixed focal plane and modulation. The relative error is $\pm 1.1\%$

where t is the exposure time, m is the laser power modulation (in %), r is the radius of the printed dot and P is derived from the maximum power density (351 kW cm^{-2}) given by the manufacturer and divided by the area of the laser spot with a diameter of $1 \mu\text{m}$ (resolution of the machine). This last calculation is only theoretical and was not yet been validated by measurements due to the complicated setup. However, the exposure dose required, as stated in the resist datasheet, is around 550 mJ cm^{-2} and it was always surpassed with the combination of the chosen parameter during the laser writing. Fig. 8, shows the effects of both plasmas on the resist mask. Mainly, due to the higher energy at a lower wavelength for the H_2 plasma (Lyman series), as depicted in Fig. 8 (b), the resist was hard baked and it was no longer possible to remove even after repeated cleaning in acetone and NMP. This is also confirmed by the absorbance coefficient of the resist, which shows a peak at a wavelength under 250 nm . In some cases, the resist hardbake occurred only at the boundary of the resist, due to the fact that this effect is strictly dependent on the previous process conditions modifying parameters such as the resist thickness. Therefore, the O_2 plasma was chosen for reliable and repeatable results as shown in Fig. 8 (a). The last evaluation was regarding the wet etching process. Using the *Keyence 3D laser scanner* as an optical profilometer, the side a and the angle α reported in the schematic in the Fig. 9 (a) were measured for each plane as shown in Fig. 9 (b).

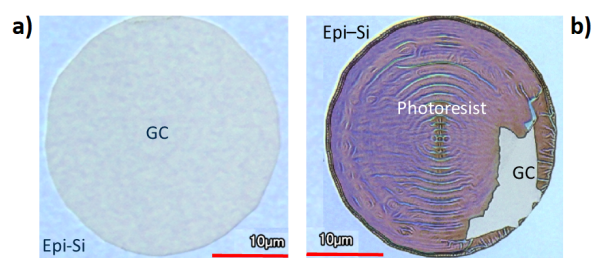


Figure 8. Comparison between two different plasmas during the dry etching process. a) effect of O_2 plasma on a circular resist pattern. Next, the resist over the GC layer was successfully removed by solvents. b) hardbake effect on the resist after H_2 plasma on a circular resist pattern.

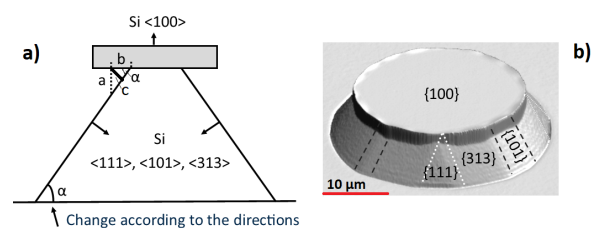


Figure 9. a) Schematic of the crystal plane section. b) 3D laser scanner image of a circle (top view) with a diameter of $31 \mu\text{m}$. The wet etching step was performed for 9 min and the absolute height obtained is $8.9 \mu\text{m}$. The investigated planes are highlighted, the other planes are symmetric [2].

Using the right-angled triangle definition:

$$c = a \cdot \cos(\alpha) \quad (2)$$

and divide by the etching time the etch-rate for each crystal plane is estimated as reported in the Tab. 1.

Table 1. The etching rate (second row), expressed in $\mu\text{m min}^{-1}$, evaluated for each crystal plane (first row).

| (100) | (111) | (313) | (101) |
|-------|-------|-------|-------|
| 0.82 | 0.1 | 0.13 | 0.15 |

Fig.10 shows a comparison between the use of KOH without isopropanol (a) and with isopropanol (b). In Fig.10(c) two problems are highlighted: the first concerning the effect of the H_2 plasma on the resist, as discussed before, and the second regarding the missing dip in HF before the KOH bath that produces hillocks on the substrate.

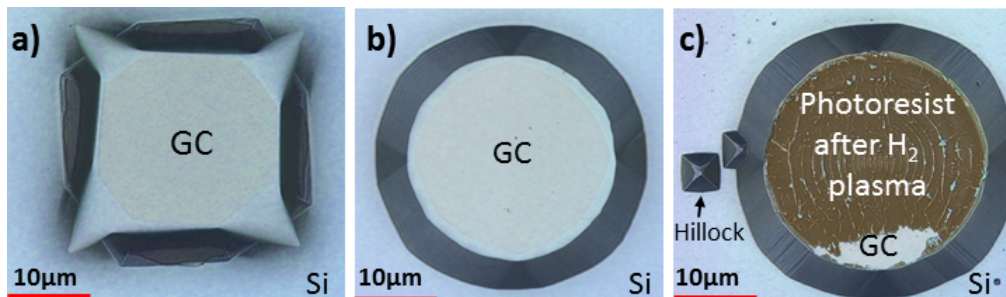


Figure 10. a) Effect of wet etching with (5M)KOH not saturated with isopropanol. b) Effect of wet etching: first HF(5%) dip for 20 sec and after (5M)KOH saturated with isopropanol. c) Effects of H_2 plasma on the resist and (5M)KOH saturated with isopropanol without a prior dip in HF(5%) and a resulting hillocks formation on the surface.

4. Conclusions

In conclusion, an easy method to pattern different shapes on (100) silicon substrates is shown. The polycrystalline GC as an etch mask for wet chemical processing offers different advantages such as excellent adhesion to silicon due to the formation of covalent bonds during the deposition, material thinness, resistance to common solvents, aggressive acids (HF) and bases (KOH), easy and quick removal by O_2 plasma. Furthermore, it is an excellent conductive material that could be directly used as a stable contact.

5. References

- [1] French P J *et al.* 1997 *Sensors and Actuators A: Physical* **62**
- [2] Barycka I *et al.* 1995 *Sensors and Actuators A: Physical* **48**
- [3] Zubel I *et al.* 2004 *Sensors and Actuators A: Physical* **115**
- [4] Zubel I *et al.* 2002 *Sensors and Actuators A: Physical* **101**
- [5] Bianco A *et al.* 2013 *Carbon* **65**
- [6] Kreupl F 2011 *MRS Proceedings* **1303**
- [7] Huebner S *et al.* 2015 *IEEE Transactions on Nuclear Science* **62**
- [8] Reinhard D K *et al.* 2004 *J. Vac. Sci. Technol. B: Microelectr. Nanom. Struct.* **22**
- [9] Stelzer M *et al.* 2017 *IEEE Journal of the Electron Devices Society* **5**
- [10] Kern W 1990 *Journal of the Electrochemical Society* **137**
- [11] Pimenta M A *et al.* 2007 *Phys. Chem. Chem. Phys.* **9**